

# Raman analysis of light-emitting porous silicon

Zhifeng Sui, Patrick P. Leong, and Irving P. Herman

Department of Applied Physics and Microelectronics Sciences Laboratory, Columbia University,  
New York, New York 10027

Gregg S. Higashi and Henryk Temkin

AT&T Bell Laboratories, Murray Hill, New Jersey 07974

(Received 21 October 1991; accepted for publication 19 February 1992)

Porous silicon that strongly emits in the visible was analyzed using Raman scattering. The spectrum peaks near  $508\text{ cm}^{-1}$ , has a width of  $\sim 40\text{ cm}^{-1}$ , and is very asymmetric. Using a model of phonon confinement, this suggests that the local structure of porous silicon is more like a sphere than a rod and has a characteristic diameter of 2.5–3.0 nm. Polarization Raman measurements suggest that the structure does not consist of a series of parallel columns.

There have been several recent reports of strong visible luminescence at room temperature from porous silicon.<sup>1,2</sup> These results have stimulated a great deal of excitement because they suggest the possibility of a Si-based optoelectronics technology. Porous silicon, which consists of a network of randomly spaced pores in silicon, is formed by electrochemical etching of a crystalline silicon wafer in concentrated hydrofluoric acid solutions under a controlled current. The pore size and porosity can vary over a wide range depending on the electrochemical parameters and the doping conditions of the initial Si wafer.<sup>3–6</sup> Electron microscopy suggests that the pores preferentially propagate in directions specified by the crystal axes<sup>7</sup> or the direction of current flow.<sup>8</sup> Because of the tremendous number of pores in the porous silicon, the surface area can become very large. Thus the amount of oxygen in the oxide layer covering the internal surface of porous silicon is very high, with one study measuring a relative concentration of  $\text{Si}:\text{O} \approx 1:0.3$ .<sup>9</sup> Light-emitting porous silicon has been fabricated by an electrochemical etch followed by a chemical etch.<sup>1,2</sup> It has been suggested that such material with high porosity (greater than 78.5%) consists of an array of separate silicon columns,<sup>1</sup> and that the emission of visible light from porous Si may be due to quantum confinement effects.<sup>1,2</sup> One study has shown that the spacing of electronic energy levels in nanometer-sized silicon islands in a  $\text{SiO}_2$  matrix may be greater than those in bulk crystalline silicon.<sup>10</sup> Therefore, an understanding of the structural and electronic properties of porous silicon is important. To help address these issues, this letter reports the first Raman analysis of light-emitting porous silicon.

Raman scattering is a nondestructive tool that is useful in the characterization of semiconductors.<sup>11</sup> Among other things, it has been used to determine grain sizes in microcrystalline materials.<sup>11–15</sup> The first-order Raman peak in *c*-Si is shifted by  $520.5\text{ cm}^{-1}$ ; it is symmetric and has a width of  $3\text{ cm}^{-1}$  (FWHM). As the grain size in microcrystalline silicon ( $\mu\text{c Si}$ ) decreases below  $\sim 200\text{ \AA}$ , the Raman shift decreases, the width increases, and the peak becomes increasingly asymmetric, with an extended tail at low frequencies.<sup>13</sup> The Raman spectrum of amorphous silicon (*a*-Si) peaks near  $480\text{ cm}^{-1}$  and is usually weak in intensity and very broad.<sup>13</sup> The first-order Raman spectra of porous silicon films made from degenerately and non-

degenerately doped silicon have been reported by Goodes *et al.*<sup>16</sup> For the degenerate material, there was a peak at  $521\text{ cm}^{-1}$  that was broader than the peak for *c*-Si and a second, weaker feature at a smaller Raman shift. The shift of this latter peak decreased to  $505\text{ cm}^{-1}$  as the density of the film decreased. Since there appears to be silicon oxide within porous silicon, it is noted that  $\text{SiO}_2$  glass has a broad Raman peak near  $430\text{ cm}^{-1}$ , while crystalline quartz has a strong, relatively sharp peak near  $464\text{ cm}^{-1}$ .<sup>17</sup>

Thick porous silicon films ( $\sim 100\text{ }\mu\text{m}$ ) were made out of float-zone *p*-type Si(001) (resistivity of  $150\text{ }\Omega\text{ cm}$ ) using techniques described by Canham.<sup>1</sup> These films were thick enough so that the underlying silicon substrate is not probed by Raman scattering. Before etching, the wafers had a minority carrier lifetime of  $\sim 4\text{ ms}$ . Band-edge photoluminescence could be readily observed at room temperature. In the etched areas very bright photoluminescence is seen, which peaks near  $6350\text{ \AA}$  and has a full width at half maximum of  $\sim 1000\text{ \AA}$  when excited by  $4880\text{ \AA}$  from an argon-ion laser. The estimated photoluminescence efficiency is  $\sim 1\%$ . Polarized Raman spectra were taken at room temperature in backscattering configuration with this  $4880\text{ \AA}$  line, using a triple monochromator for dispersion and an intensified photodiode array for detection. The resolution of the spectra is typically less than  $1\text{ cm}^{-1}$ . The laser power used in Raman analysis is  $\sim 1\text{ mW}$  and the spot size on the sample is  $\sim 10\text{ }\mu\text{m}$ . Because of the low thermal conductivity of porous silicon and the temperature dependence of the Raman shifts and linewidths, care was taken to avoid laser heating of the sample.

Raman spectra of the light-emitting porous silicon were collected in six polarization configurations to help identify the structure. With the laser impinging normal to the surface,  $z(x,y)\bar{z}$  and  $z(x,x)\bar{z}$  spectra were taken. As expected, Raman spectra were seen in the former and were not seen in the latter configuration from the parts of the *c*-Si(001) surface that had not been etched. Unpolarized spectra were also collected. Backscattered spectra of the porous silicon film were also taken with the laser impinging normal to the edge of the porous silicon film/*c*-Si wafer in the middle of the film. Using the same crystal coordinates, these correspond to  $x(y,y)\bar{x}$ ,  $x(y,z)\bar{x}$ ,  $x(z,z)\bar{x}$ , and  $x(z,y)\bar{x}$ .

The Raman spectrum of a light-emitting porous silicon film is shown in Fig. 1. It is plotted again in Fig. 2 with the

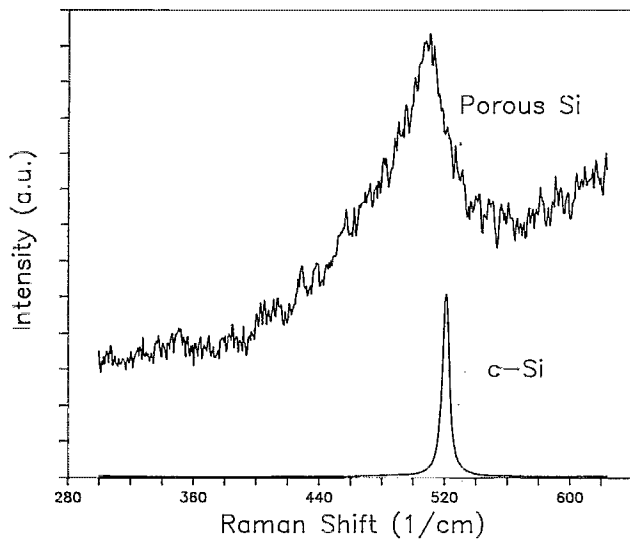


FIG. 1. The unpolarized Raman spectrum of a thick light-emitting porous silicon film, with the Raman spectrum of *c*-Si shown for comparison. The background in the porous silicon spectrum is due to the tail of the photoluminescence spectrum.

background subtracted; this background was verified to be from the high energy side tail of the photoluminescence spectrum. As indicated in Fig. 3, the Raman shifts vary from 508.0 to 510.1  $\text{cm}^{-1}$  and the widths from 32 to 42  $\text{cm}^{-1}$  (FWHM) for the different polarizations and probing positions. Also, the peaks are very asymmetric. These parameters of these spectra lie between those of  $\mu\text{c}$ -Si and  $\alpha$ -Si. No peak from the *c*-Si substrate is seen in any of the spectra. Essentially, the same Raman spectrum is seen using each of the six polarization configurations, with the relative peak intensities varying by a factor of  $\sim 2$ . Since spectra taken on the top and in the middle of the edge of the film are almost the same, the structure of the film is fairly homogeneous.

In an ideal crystal translational symmetry leads to plane wave phonon eigenstates. The phonons involved in first-order Raman scattering have  $\mathbf{q} = 0$  and are at the cen-

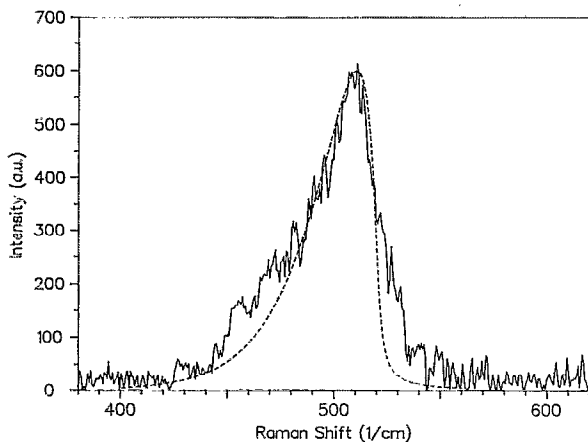


FIG. 2. The background-subtracted Raman spectrum of porous silicon from Fig. 1 compared with the spectrum calculated for a sphere with diameter  $L = 29 \text{ \AA}$  (dashed line).

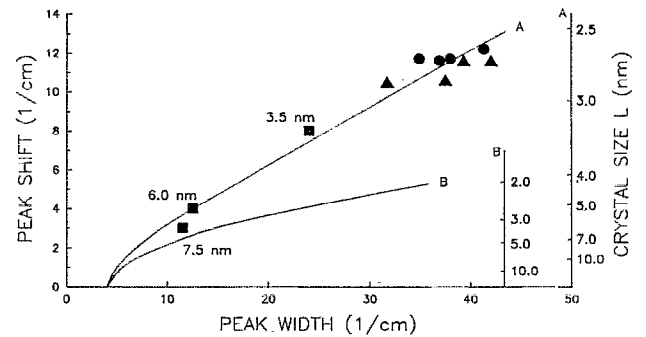


FIG. 3. The calculated relationship between the Raman width, the decrease of the Raman shift relative to the shift in *c*-Si, and the nanocrystal size  $L$  for spherically shaped nanocrystals (curve A,  $L$  is the sphere diameter) and cylindrically shaped nanocrystals (curve B,  $L$  is the cylinder diameter). The triangles [circles] are the experimental data with perpendicular [parallel] incident and Raman polarizations, such as  $z(x,y)\bar{z}$  [ $x(x,x)\bar{x}$ ] with respect to the unetched Si wafer, taken on different places on and along the edge of the film. The squares are Raman data for  $\mu\text{c}$ -Si from Ref. 13, with the crystallite dimensions listed from x-ray diffraction.

ter of the Brillouin zone ( $\Gamma$  point). However, disorder or finite-size effects may partially or completely relax “momentum” conservation, leading to a downshift and broadening of the Raman peak.<sup>12</sup> A quantitative model was developed by Richter *et al.*<sup>12</sup> and was later improved by Campbell and Fauchet<sup>14</sup> to estimate the average size (or correlation length)  $L$  of the nanocrystals from the Raman spectrum. For spherical nanocrystals  $L$  is the diameter. Using this model, the first-order Raman spectrum  $I(\omega)$  is

$$I(\omega) \propto \int \exp(-q^2 L^2 / 4) \frac{d^3 q}{[\omega - \omega(q)]^2 + (\Gamma/2)^2} \quad (1)$$

where  $q$  is expressed in units of  $2\pi/a$  and  $L$  is in units of  $a$ , with  $a = 0.357 \text{ nm}$  being the lattice constant of silicon.  $\Gamma$  is the natural linewidth ( $\sim 4 \text{ cm}^{-1}$  for *c*-Si at room temperature including instrumental contributions) and  $\omega(q)$  is the dispersion relation for optical phonons in *c*-Si. To calculate the line shape, the analytic form  $\omega(q) = A - Bq^2$ , with  $A = 520.5 \text{ cm}^{-1}$  and  $B = 120 \text{ cm}^{-1}$  is used, which reproduces the dispersion relation for LO phonons along [001] in Si quite well. Since LO and TO phonons are degenerate at (and very near) zone center and the phonons contributing to the integral are from and near zone center if  $L \gg a$ , this analytic dispersion relation should be a good approximation for  $L \gg a$ . [Only LO phonons are important for backscattering from *c*-Si (001).] A spherically symmetric Brillouin zone is assumed here.

Equation (1) assumes spherical crystal grains, and has been confirmed in Refs. 13 and 14 for the three-dimensional phonon confinement found in  $\mu\text{c}$ -Si. Because of the suggestion of a rodlike geometry in Ref. 1, the possibility of very long cylindrically shaped structures, whose length  $\gg$  diameter, is also considered.<sup>14</sup> Because of the conservation of momentum along the cylindrical axis, the integral in Eq. (1) becomes two dimensional (cylindrical coordinates) rather than three dimensional (spherical co-

ordinates), as in Ref. 14. This extension of Eq. (1) to two dimensions has not yet been confirmed experimentally.

Figure 2 shows the good agreement of a typical Raman spectrum of the light-emitting porous silicon with the calculated spectrum for a sphere with diameter  $L = 2.9$  nm. Figure 3 gives the relationship between the Raman width, Raman shift with respect to *c*-Si, and the crystal size, which was calculated here by using Eq. (1) for spherical and cylindrical nanocrystals. The data for light-emitting porous silicon taken at different points for different polarizations are plotted. These Raman data lie along the spherical grain model, and suggest that local structure is more like a sphere, with a diameter between 2.5 and 3.0 nm, than like a rod. For reference, published data for crystallite sizes in  $\mu\text{c}$  Si from *x*-ray diffraction and Raman scattering are also indicated in Fig. 3.<sup>13,14</sup> The Raman spectra measured here are very well fit by the asymmetric spectra predicted by this model (Fig. 2), suggesting that the distribution of the crystalline sizes has a single peak, which is relatively narrow.

If the silicon atoms remaining in the structure after etching still maintain the local symmetry of the *c*-Si lattice, then the Raman polarization selection rules for photons in the silicon structure would be the same as those for *c*-Si. However, because of refraction of light into and out of the silicon regions, the experimentally observed polarization signals may be different. If the porous structure consisted of an array of columns, the incident laser would be transmitted into the material along the crystal axes and the polarized spectra would vanish in some configurations [such as  $z(x,x)\bar{z}$ ]. However, if the porous structure was highly irregular, then the light that is transmitted into the structure would be greatly refracted. In this case, the different experimental polarization configurations would give roughly the same signal intensities. The latter possibility with the irregular structure is suggested by these experiments.

After the submission of this work, the authors learned of another Raman study of light emitting porous silicon.<sup>18</sup> When luminescence peaked near 1.6 eV, the Raman spectrum in Ref. 18 had a single peak near  $519\text{ cm}^{-1}$ , while for luminescence near 1.9 eV there were peaks near 518 and  $510\text{ cm}^{-1}$ . This latter spectrum was attributed to LO/TO phonon splitting, and led the authors to conclude that

there is quantum confinement with a characteristic dimension of 2–3 nm. The shape of the local structure was not determined. Though the measurements on thick samples reported in the current study lead to a similar conclusion about the confinement dimensions, the Raman spectra presented here have a single peak that is similar to their  $510\text{ cm}^{-1}$  peak and do not suggest LO/TO phonon splitting. As in Ref. 18, no evidence of amorphous silicon is seen here.

In summary, the Raman spectrum from a thick film of light-emitting porous silicon resembles that of  $\mu\text{c}$  Si with a grain size between 2.5 and 3.0 nm. The local structure seems to be roughly spherical and not rodlike. The shape and the polarization properties of these Raman spectra suggest that these porous films are not ordered arrays of silicon columns.

The authors at Columbia would like to acknowledge support by the Joint Services Electronics Program under Contract DAAL03-91-C-0016 and by the Office of Naval Research.

<sup>1</sup>L. T. Canham, Appl. Phys. Lett. 57, 1046 (1990).

<sup>2</sup>A. Halimaoui, C. Oules, G. Bomchil, A. Bsiesy, F. Gaspard, R. Herino, M. Ligeon, and F. Muller, Appl. Phys. Lett. 59, 304 (1991).

<sup>3</sup>G. Bomchil, A. Halimaoui, and R. Herino, Appl. Surf. Sci. 41/42, 604 (1989).

<sup>4</sup>R. Herino, G. Bomchil, K. Barla, C. Bertrend, and J. L. Ginoux, J. Electrochem. Soc. 134, 1994 (1987).

<sup>5</sup>G. Bomchil, A. Halimaoui, and R. Herino, Microelectron. Eng. 8, 293 (1988), and references therein.

<sup>6</sup>P. C. Searson, Appl. Phys. Lett. 59, 832 (1991).

<sup>7</sup>S.-F. Chuang, S. D. Collins, and R. L. Smith, Appl. Phys. Lett. 55, 675 (1989).

<sup>8</sup>M. I. J. Beale, N. G. Chew, M. J. Uren, A. G. Cullis, and J. D. Benjamin, Appl. Phys. Lett. 46, 86 (1985).

<sup>9</sup>G. Bai, K. H. Kim, and M. Nicolet, Appl. Phys. Lett. 57, 2247 (1990).

<sup>10</sup>D. J. Dimaria, J. R. Kirtley, E. J. Pakulis, D. W. Dong, T. S. Kuan, F. L. Pesavento, N. Theis, and J. A. Curto, J. Appl. Phys. 56, 401 (1984).

<sup>11</sup>F. H. Pollak and R. Tsu, SPIE Proc. 452, 26 (1983).

<sup>12</sup>H. Richter, Z. P. Wang, and L. Ley, Solid State Commun. 39, 625 (1981).

<sup>13</sup>Z. Iqbal and S. Veprek, J. Phys. C: Solid State Phys. 15, 377 (1982).

<sup>14</sup>I. H. Campbell and P. M. Fauchet, Solid State Commun. 58, 739 (1986).

<sup>15</sup>A. Tu and P. D. Persans, Mater. Res. Soc. Symp. Proc. 206, 97 (1991).

<sup>16</sup>S. R. Goodes, T. E. Jenkins, M. I. J. Beale, J. D. Benjamin, and C. Pickering, Semicond. Sci. Technol. 3, 483 (1988).

<sup>17</sup>P. McMillan, in *The Physics and Technology of Amorphous SiO<sub>2</sub>*, edited by R. A. B. Devine (Plenum, New York, 1988), p. 63.

<sup>18</sup>R. Tsu, H. Shen, and M. Dutta, Appl. Phys. Lett. 60, 112 (1992).